

in dislocations of different types is obviously of paramount interest. It is our hope that this can be established by further experimental and theoretical study.

#### ACKNOWLEDGMENT

I wish to thank Dr. A. W. Overhauser for his continued interest in this work.

#### APPENDIX

The Lagrangian,  $L$ , of a set of kinks at positions,  $x_i$ , is

$$L = \frac{1}{2} m_k \sum_i \dot{x}_i^2 - \frac{1}{2} \sum_{i,j, (i \neq j)} U(|x_i - x_j|). \quad (\text{A1})$$

We wish to determine the time development of the macroscopic density,  $n(x)$ . Since

$$n(x) = \sum_i \delta(x - x_i), \quad (\text{A2})$$

apart from self-energy terms, which we can ignore, the total potential energy,  $V$ , may also be rewritten as

$$V = \frac{1}{2} \int_{-L/2}^{L/2} dx \int_{-L/2}^{L/2} dx' U(|x - x'|) n(x) n(x'). \quad (\text{A3})$$

Our aim will be to express the kinetic energy in terms of similar collective variables, and hence derive the equations of motion.

We introduce the complex Fourier transform,  $n_q$ , by means of the relation

$$n_q = L^{-1/2} \int_{-L/2}^{L/2} n(x) e^{-iqx} dx. \quad (\text{A4})$$

That is, from (A2),

$$n_q = L^{-1/2} \sum_i e^{-iqx_i}. \quad (\text{A5})$$

Then, the momentum,  $\Phi_{-q}$  say, canonically conjugate to  $n_q$  is given by

$$\Phi_{-q} = \partial L / \partial \dot{n}_q. \quad (\text{A6})$$

But since

$$p_i = \frac{\partial L}{\partial \dot{x}_i} = \sum_q \Phi_{-q} \frac{\partial \dot{n}_q}{\partial \dot{x}_i}, \quad (\text{A7})$$

we find, after differentiating (A5) with respect to time, that

$$p_i = -iL^{-1/2} \sum_q \Phi_{-q} q e^{-iqx_i}. \quad (\text{A8})$$

Hence, the kinetic energy,  $T$ , of the system is

$$\begin{aligned} T &= \sum_i (p_i^2 / 2m_k) \\ &= (1/2m_k L^{1/2}) \sum_{q,q'} q q' \Phi_{-q} \Phi_{q'} n_{q-q'}, \end{aligned} \quad (\text{A9})$$

or

$$T = (1/2m_k) \int_{-L/2}^{L/2} n(x) (\partial \Phi / \partial x)^2 dx, \quad (\text{A10})$$

where

$$\Phi_q = L^{-1/2} \int_{-L/2}^{L/2} \Phi(x) e^{-iqx} dx. \quad (\text{A11})$$

Equation (A10) will be recognized as the kinetic energy of a fluid when expressed in terms of a velocity potential  $\Phi(x)/m_k$ . The equations of motion for  $n$  and  $\Phi$  may be found from the Hamiltonian,  $H = T + V$ . After the substitution  $m_k v(x) = \partial \Phi / \partial x$ , the latter yield Eqs. (2) and (3) of the text.

## Nuclear Magnetic Resonance in $\text{UAl}_2$

A. C. GOSSARD, V. JACCARINO, AND J. H. WERNICK  
Bell Telephone Laboratories, Murray Hill, New Jersey

(Received May 15, 1962)

The nuclear magnetic resonance of  $\text{Al}^{27}$  in  $\text{UAl}_2$  has been observed in the range of temperatures 4–300°K. Large Knight shifts ( $K$ ) were found with a temperature dependence not of a Curie-Weiss type. This behavior and the temperature independence of the linewidth, when considered in conjunction with susceptibility ( $\chi$ ) measurements, indicate (1) no localization of the magnetization of the U (5*f* and/or 6*d*) electrons and (2) no magnetic ordering exists. These results are contrasted with those obtained on the isostructural  $\text{XAl}_2$  ( $X$ =rare-earth ion) metals. Using a simple model, certain features of the band structure and the effective exchange interaction between itinerant *f* and *s* electrons may be deduced. From the extrapolated limit of the linear  $K$  vs  $\chi$  curve a large positive temperature-independent contribution to  $\chi$  is obtained which is attributable to the Kubo-Obata orbital paramagnetism to be expected in metals with unfilled degenerate bands.

#### INTRODUCTION

**E**XPERIMENTAL evidence of an appreciable exchange interaction between the localized spin moments of the rare-earth ions and the conduction

electrons has been obtained from nuclear magnetic resonance (NMR) studies<sup>1</sup> of the  $\text{XAl}_2$  intermetallic

<sup>1</sup> V. Jaccarino, B. T. Matthias, M. Peter, H. Suhl, and J. H. Wernick, Phys. Rev. Letters 5, 251 (1960).

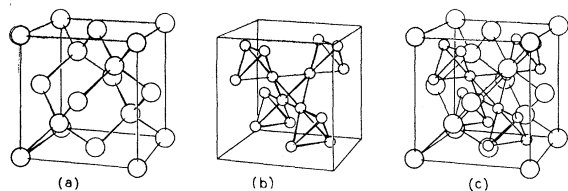


FIG. 1. The cubic Laves phase; fcc C15 structure type, lattice constant  $a=7.795 \text{ \AA}$ . (a) The uranium sublattice; (b) the aluminum sublattice; (c) the composite  $\text{UAl}_2$  structure.

compounds (see Fig. 1) ( $X \equiv$  rare earth). In the paramagnetic state<sup>2</sup> of the magnetically dense metals (e.g.,  $\text{GdAl}_2$ ) the  $\text{Al}^{27}$  NMR exhibits large temperature and field dependent shifts, while in the dilute metals (e.g.,  $\text{Gd}_{0.001}\text{La}_{0.999}\text{Al}_2$ ) the  $\text{La}^{139}$  and  $\text{Al}^{27}$  NMR are broadened but unshifted relative to their corresponding resonances in the nonmagnetic  $\text{LaAl}_2$ .<sup>3</sup> These observations may be accounted for by the spatially varying polarization induced in the conduction band by the exchange interaction between a localized distribution of spin magnetization ( $4f$  shell of the rare-earth ion) and the spin moments of the conduction electrons.<sup>4,5</sup>

It is of interest then to include in these studies the behavior of the corresponding actinide-aluminum metals. In particular in the  $5f$  shell metals,  $\text{UAl}_2$ ,  $\text{NpAl}_2$ , and  $\text{PuAl}_2$  form the isostructural cubic Laves phase (Fig. 1) whereas  $\text{ThAl}_2$  does not.<sup>6</sup> In the first three metals problems associated with radioactivity and availability have necessitated our confining our attention to  $\text{UAl}_2$ .

### EXPERIMENTAL

The samples were prepared from the metallic elements U (purity 99.95%) and Al (purity 99.999%) by induction heating of stoichiometric quantities in quartz crucibles in an argon atmosphere. X-ray powder patterns indicated that the ingots were free of any second phase. For the NMR experiments the samples were crushed in an agate mortar in an argon filled dry box ( $\text{UAl}_2$  is quite pyrophoric!) and sieved through a 400-mesh screen.

We have examined the NMR of  $\text{Al}^{27}$  ( $I=5/2$ ) in  $\text{UAl}_2$  in the temperature range from 4.2 to 300°K in fields varying from 7 to 14 kOe using a Varian NMR spectrometer. An observed  $\text{Al}^{27}$  NMR absorption derivative spectrum is shown in Fig. 2. The large central peak is attributed to the ( $m_I = +1/2 \leftrightarrow m_I = -1/2$ ) transitions, while the smaller satellite peaks are associated with other  $\Delta m_I = \pm 1$  transitions, whose frequencies are shifted in first order by a nuclear electric quadrupole interaction between the nuclear quadrupole moment

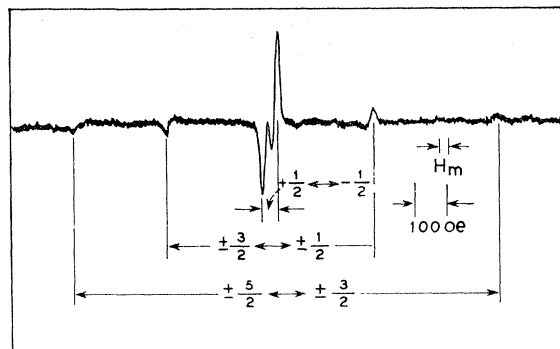


FIG. 2. A recording of the derivative of the  $\text{Al}^{27}$  NMR absorption spectrum as a function of field in  $\text{UAl}_2$  at 20°K in a magnetic field of approximately 14kOe showing the structure arising from the nuclear electric quadrupole interaction.

$Q$  and the axial electric field gradient  $q$ . (The point symmetry of the aluminum sites is trigonal  $\bar{3}m$ .) The frequency difference between the ( $m_I \leftrightarrow m_I - 1$ ) transition and the ( $1/2 \leftrightarrow -1/2$ ) transition to first order is  $(2m_I - 1)(3 \cos^2 \theta - 1)[3e^2qQ/8I(2I - 1)\hbar]$ , where  $\theta$  is the angle between the trigonal symmetry axis at the Al site and the applied magnetic field. Although in powdered samples  $\theta$  assumes all values between 0 and  $\pi$ , sharp peaks in the power absorbed occur at frequencies corresponding to  $\theta = \pi/2$ .<sup>7</sup> These peaks result from the singularity in the number of nuclei per unit frequency at  $\theta = \pi/2$  and are seen in the observed spectrum as the satellite lines. The spacing between the innermost satellites is  $3e^2qQ/2I(2I - 1)\hbar = 3e^2qQ/20\hbar$ . The observed spacing, after correction for dipolar and magnetic modulation broadening, then corresponds to  $e^2qQ/\hbar = 4.620 \text{ Mc/sec}$ . The quadrupole interaction also affects the central ( $+1/2 \leftrightarrow -1/2$ ) transition's frequency and linewidth, and this effect must be considered before one can find the NMR shifts which are truly *magnetic* in origin. Although there is no first-order quadrupolar shift of the central line, a second-order shift of the frequency

$$-\frac{9}{64} \frac{2I+3}{4I^2(2I-1)} \frac{(e^2qQ)^2}{\hbar^2\nu_0} (1-9\cos^2\theta)(1-\cos^2\theta)$$

occurs, where  $\nu_0$  is the frequency of the unshifted line. In a powder, peaks in the power absorbed occur at the maximum and minimum frequencies of this distribution,<sup>8</sup> which again correspond to singularities in the number of nuclei per unit frequency and, for  $I=5/2$ , occur at shifts of

$$+(9/800)(e^2qQ)^2/\hbar^2\nu_0 \text{ and } -(16/800)(e^2qQ)^2/\hbar^2\nu_0.$$

To determine the center of the quadrupole broadened central line, it was thus necessary to find the point

<sup>2</sup> V. Jaccarino, J. Appl. Phys. **32**, 1025 (1961).  
<sup>3</sup> A. C. Gossard, V. Jaccarino, and J. H. Wernick, J. Phys. Soc. Japan **17**, Suppl. B-1, 91 (1962).

<sup>4</sup> K. Yosida, Phys. Rev. **106**, 893 (1957).

<sup>5</sup> R. E. Behringer, J. Phys. Chem. Solids **2**, 209 (1957).

<sup>6</sup> W. B. Pearson, *Lattice Spacings and Structure of Metals and Alloys* (Pergamon Press, New York, 1958).

<sup>7</sup> W. A. Nierenberg and N. F. Ramsey, Phys. Rev. **72**, 1075 (1947).

<sup>8</sup> B. T. Feld and W. E. Lamb, Phys. Rev. **67**, 15 (1945).

which is located 16/25 of the distance from the low-frequency to the high-frequency derivative peaks.

Another possible source of linewidth of the central component is an anisotropic Knight shift. In the presence of combined second-order quadrupole broadening and anisotropic Knight shift broadening, the linewidth for  $I=5/2$  (after subtracting nuclear dipole and field modulation contributions) would be<sup>9,10</sup>

$$\delta\nu = \frac{1}{32} \frac{(e^2qQ)^2}{h^2\nu_0} - \frac{5}{9}(K_{11}-K_1)\nu_0 + \frac{200}{81} \frac{(K_{11}-K_1)^2\nu^3/h^2}{(e^2qQ)^2}, \quad (1)$$

where  $K_{11}$  and  $K_1$  are the Knight shifts at  $\theta=0$  and  $\pi/2$ , respectively. In order to evaluate the importance of the anisotropic Knight shift contribution to the linewidth, we have plotted in Fig. 3  $\nu_0\delta\nu$  vs.  $\nu_0^2$  for a number of different frequencies. Equation (1) shows (neglecting momentarily the third term) that the slope of the resulting plot measures the anisotropy of the Knight shift, and that the  $\nu_0\delta\nu$  intercept at  $\nu_0^2=0$  is proportional to the square of the quadrupole interaction. The quadrupole interaction deduced in this way agrees well with that obtained from measuring the first-order satellite splittings, while the small slope indicates that  $K_{11}-K_1$  is less than 0.03% and is thus a negligible linewidth mechanism. The third term in Eq. (1) is less than 0.1% of the observed linewidth and was justifiably neglected.

The fractional shift  $K$  of the  $\text{Al}^{27}$  NMR is given as a function of temperature in Fig. 3. (The position of the  $\text{Al}^{27}$  NMR in a Cr-doped  $\text{KAlSO}_4$  solution is used as a reference with respect to which  $K$  is measured.) Though the magnitude and temperature dependence of  $K$  is considerably in excess of that which is observed in, say, Al metal<sup>7</sup> there is nevertheless no evidence for a Curie-Weiss law behavior as was found in the rare-earth  $\text{Al}_2$

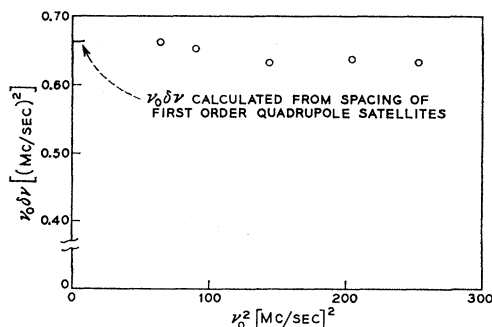


FIG. 3. A plot of  $\nu_0\delta\nu$  vs  $\nu_0^2$  for the  $(1/2 \leftrightarrow -1/2)\text{Al}^{27}$  NMR in  $\text{UAl}_2$  at 20°K.

<sup>9</sup> W. H. Jones, Jr., and F. J. Milford, Phys. Rev. **125**, 1259 (1962).

<sup>10</sup> R. G. Barnes, W. H. Jones, Jr., and T. P. Graham, Phys. Rev. Letters **6**, 221 (1961).

metals. Furthermore, at the lowest temperature (4.2°K) the resonance is still observable and has, in fact, not broadened. This indicates no ferromagnetic or antiferromagnetic ordering has occurred. To check this conclusion the susceptibility has been measured between 1.4 and 300°K by Williams and Sherwood.<sup>12</sup> Their results are shown in Fig. 4 as well. No indication of ordering was found in their measurements.

If we plot  $K$  vs  $\chi$  we find a linear relation to hold. (See Fig. 4.) The extrapolated limit at  $K=0$  corresponds to a susceptibility  $\chi_0 = 2.1 \times 10^{-6}$  emu/g.

## INTERPRETATION AND DISCUSSION

We present here an interpretation of these results and their relevance to the previously reported work on the rare-earth  $\text{Al}_2$  metals. Three distinct features of the NMR and susceptibility measurements are apparent and will be discussed separately: (1) band character of the U 5f and 6d electrons, (2) the degree of admixture of Al 3s wave functions into the U 6d and 5f bands or,

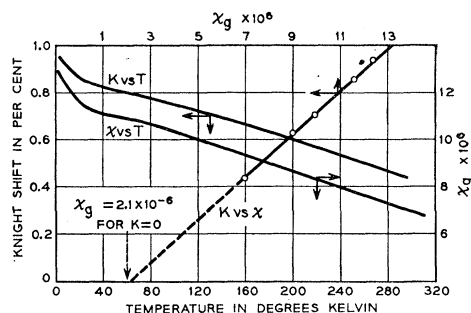


FIG. 4. A plot of Knight shift vs temperature, susceptibility vs temperature and Knight shift vs susceptibility. (The arrows on each curve indicate the appropriate axes).

alternatively, the exchange interaction between itinerant  $f$  and  $s$  electron bands, and (3) evidence for a large contribution to the susceptibility arising from the temperature-independent orbital paramagnetism of the partially filled degenerate 5f band.

## 1. Band Character of the Uranium 5f and 6d Electrons in $\text{UAl}_2$

The free uranium atom has the atomic configuration  $5f^36d^17s^2$  outside the closed radon core. Relative to the rare-earth 4f electrons the wave functions of the 5f electrons are rather extended<sup>13</sup> and, in uranium metal,

<sup>11</sup> For a discussion of the Knight shifts in metals see W. D. Knight, in *Solid State Physics*, edited by F. Seitz and D. Turnbull (Academic Press Inc., New York, 1956), Vol. 2.

<sup>12</sup> H. J. Williams and R. C. Sherwood (private communication).

<sup>13</sup> A graphic demonstration of the relative spatial extent of the 4f and 5f wave functions is found in the electron paramagnetic resonance of  $\text{Nd}^{3+}$  and  $\text{U}^{3+}$  as impurities in a  $\text{CaF}_2$  lattice. In the  $\text{U}^{3+}$  case the resonance exhibits a  $F^{10}$  hfs whereas the  $\text{Nd}^{3+}$  resonance is devoid of this effect. The  $F^{10}$  hfs is known to occur because of the overlap of  $f$  wave functions with the F 2s wave function. B. Bleaney, P. M. Llewellyn, and D. A. Jones, Proc. Phys. Soc. (London) **B69**, 858 (1956).

for example, we may expect appreciable band character for the  $5f$  electrons whereas in Gd metal we know the  $4f$  electrons to be comparatively localized with small overlap between adjacent Gd atoms. The electronic properties of the actinide metals uranium, plutonium and neptunium reflect this distinction.

Ridley<sup>14</sup> has calculated wave functions for body-centered cubic uranium metal by determining the Hartree self-consistent field for four different atomic configurations using the Wigner-Seitz boundary conditions. For the configuration  $(5f^2)(6d^2)(7s^2)$ , for example, she has found the bandwidths of the  $f$ ,  $d$ , and  $s$  functions to be in the ratio 1:9.8:22.7. Friedel<sup>15</sup> in his treatment of the  $\alpha$ ,  $\beta$ , and  $\gamma$  phases of uranium metal has proposed that, in addition to the wide  $7s$  band, there is a hybrid  $5f-6d$  band with appreciable structure in the density of states vs. energy curve. For point of reference his  $n(E)$  vs  $E$  curve for  $\alpha$  uranium is shown in Fig. 5(a).

Undoubtedly the band structure of  $\text{UAl}_2$  will be still more complex than that of U but certain qualitative features immediately suggest themselves and will be useful in the discussion of the NMR and susceptibility results. We propose that the band structure of  $\text{UAl}_2$  may be schematicized by an  $n(E)$  vs.  $E$  curve as is given in Fig. 5(b): to wit, a very wide  $7s$  band, a somewhat narrower  $6d$  band, and a very narrow  $5f$  band. The three intersections with the Fermi surface are indicated. The numbers immediately under the band label for each  $n(E)$  curve suggest a range of occupation numbers for the filled parts of the band with the proviso that a total of 6 electrons per uranium atom are to be accommodated in the three bands. As the  $d$  and  $f$  bands require a total of 10 and 14 electrons, respectively, to be filled the designated narrow peaks in the density-of-states curve should be considered as sub-bands, to fill which perhaps only 2 to 4 electrons per atom are required. In any case, the comparative complexity of the structure and the symmetry properties of the  $f$  and  $d$  wave functions will almost certainly lead to considerable structure in the respective  $n(E)$  curves. No detailed significance is to be attached to the shape of the  $f$  and  $d$  band  $n(E)$  curves or their relative positions, either with respect to each other or to the  $7s$  band curve.

### 2a. Admixture of Al 3s Wave Function into the Uranium Band Wave Functions

Since no evidence for localized  $U$  spin moments exists in  $\text{UAl}_2$  we are led to interpret the Knight shift vs susceptibility relation using a band model. A scheme for doing this has been given in the case of the  $\text{V}_3\text{X}$  intermetallic compounds<sup>16</sup> and we may adapt this procedure to  $\text{UAl}_2$ . Let us suppose that the susceptibility arises from three separate intersections of the Fermi surface

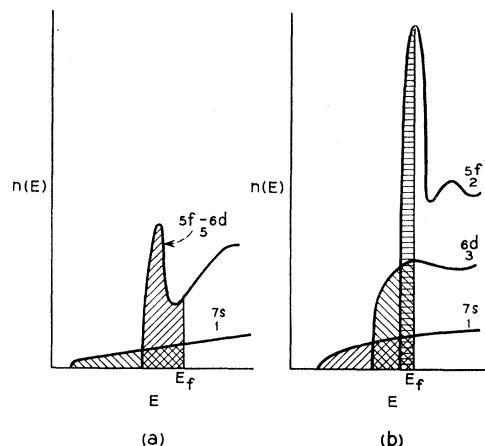


FIG. 5. Schematic density-of-states vs energy curves for (a)  $\alpha$ -U (after Friedel, see reference 15), (b)  $\text{UAl}_2$ . The numbers of electrons in the filled parts of the bands are indicated under the band labels.

with the  $7s$ ,  $6d$ , and  $5f$  band, that is  $\chi = \chi_s + \chi_d + \chi_f$ , with  $\chi_f$  being temperature dependent as a result of the rapid variation in the  $n(E)$  curve in the vicinity of  $E_F$  for the  $5f$  band and  $\chi_s + \chi_d$  being temperature independent. Furthermore, let us assume a certain fraction  $f_{3s,7s}$ ,  $f_{3s,6d}$ , and  $f_{3s,5f}$  of the Al 3s wave function to be admixed into the  $7s$ ,  $6d$ , and  $5f$  bands ( $f_{3s,7s} + f_{3s,6d} + f_{3s,5f} = 1$ ). Then the Knight shift of the Al may be expressed as

$$K_{\text{Al}} = \alpha\chi_s + \beta\chi_d + \gamma\chi_f, \quad (2)$$

with

$$\alpha = (M_0/2\mu_B)(2M_{\text{Al}} + M_{\text{U}})\xi H_{\text{HF}} f_{3s,7s}, \quad (3)$$

$$\beta = (M_0/2\mu_B)(2M_{\text{Al}} + M_{\text{U}})\xi H_{\text{HF}} f_{3s,6d}, \quad (4)$$

$$\gamma = (M_0/2\mu_B)(2M_{\text{Al}} + M_{\text{U}})\xi H_{\text{HF}} f_{3s,5f}, \quad (5)$$

where  $H_{\text{HF}}$  is the hyperfine field for an Al 3s electron,  $M_{\text{Al}}$  and  $M_{\text{U}}$  are the atomic weights of Al and U,  $M_0$  = mass of unit atomic weight,  $\mu_B$  is the Bohr magneton, and  $\xi = [|\Psi(0)|^2]_{\text{metal}}/[|\Psi(0)|^2]_{\text{atom}}$ . Since only  $\chi_{5f}$  is temperature dependent, the slope of the  $K$  vs  $\chi$  plot yields  $\gamma$  directly. Using Knight's value for the corrected hyperfine interaction constant  $A(3s)$  for Al in Al metal  $A(3s) = 0.0948 \text{ cm}^{-1}$ , corresponding to a hyperfine field  $H_{\text{HF}} = 2.54 \times 10^6 \text{ Oe}$ , and our measured value of  $\Delta K/\Delta\chi = 1.1 \times 10^3/(\text{emu/g})$  we have  $f_{3s,5f} = (1/\xi) \times 1.65 \times 10^{-2}$ . For an assumed value of  $\xi = 0.6$  we find  $f_{3s,5f} = 2\%$  which appears to be a very reasonable admixture parameter. Neither  $\alpha$  nor  $\beta$  is determined unambiguously from the data. We will discuss this point in the last section.

### 2b. Exchange Interaction Between Itinerant $f$ and Itinerant $s$ Electrons

An apparently alternative explanation of the observed relation between  $K$  and  $\chi$  may be had from assuming an  $s$ - $f$  exchange interaction between the two

<sup>14</sup> E. C. Ridley, Proc. Roy. Soc. London (London) A247, 199 (1958).

<sup>15</sup> J. Friedel, J. Phys. Chem. Solids 1, 178 (1956).

<sup>16</sup> A. M. Clogston and V. Jaccarino, Phys. Rev. 121, 1357 (1961).

*itinerant* electron systems. This problem has been formulated for the  $d$  group metals by Shimizu<sup>17</sup> and somewhat more generally by Clogston.<sup>18</sup> In analogy with the rare-earth *localized*  $4f$  electron-conduction  $6s$  electron exchange interaction we may treat the  $5f$  electrons in a tight binding approximation in which the exchange interaction is given by

$$-\sum_{kk'} J_{kk'} \mathbf{S}_{k'}^s \mathbf{S}_{k'}^s,$$

where  $\mathbf{S}_{k'}^s$  and  $\mathbf{S}_{k'}^s$  are the spin operators and  $J_{kk'}$  is the exchange integral between  $5f$  and  $7s$  electrons with wave vectors  $k$  and  $k'$ , respectively. (The  $s$  conduction band is assumed to have  $7s$  character at the U site and  $3s$  character at the Al site.) The order of magnitude of  $J_{kk'}$  is presumed to be the free atom  $J_{5f,7s}$  divided by the number of uranium lattice points  $N$ .

Again, the large temperature-dependent  $\chi$  would result from a high density of states at  $E=E_F$  in the relatively narrow  $5f$  band and enhanced by the exchange interaction between the  $f$  electrons. If the magnetization of the  $s$  band is much smaller than that of the  $f$  band and, in the absence of  $s$ - $f$  exchange, initially temperature independent, then it is easy to show from the expressions for the mean magnetization in the two bands, in the presence of exchange, that

$$\chi_s = \chi_s^0 (1 + \lambda \chi_f^0), \quad (6)$$

and correspondingly

$$K_s = K_s^0 (1 + \lambda K_f^0), \quad (7)$$

where  $\lambda = J_{5f-7s}/Ng_f g_s \mu_B^2$  is the "molecular field" constant and  $\chi_s^0$  and  $\chi_f^0$  are the unenhanced susceptibilities. The slope  $dK_s/d\chi_f^0 = \lambda K_s^0$  may be used to determine  $J_{5f-7s}$ . Now  $g_s$  will be close to the free-electron  $g$  value, but  $g_f$  may reflect the absence of complete quenching of the orbital angular momentum, because of the large value of the spin-orbit coupling in heavy atoms, and deviate appreciably from  $g_s$ .<sup>19</sup> The extrapolated  $K$  vs  $\chi$  curve does *not* have a positive intercept on the  $K$  axis, for reasons we will discuss in the next section, and we cannot deduce a value of  $K_s^0$  as a consequence. Nevertheless, we may assume that  $K_s^0$  is similar to the values found in the rare-earth aluminum metals; namely  $K_s^0 \cong 0.1\%$ . With this value for  $K_s^0$  and  $g_f \cong g_s = 2.0$  we find  $J_{5f-7s} \cong +0.6$  ev.

In Table I, we give a comparison of certain properties of the Al NMR in three  $XAl_2$  metals. For the rare-earth metals it is to be noted that the polarization in the conduction band at the aluminum site is opposite to that of the spin magnetization at the rare-earth site. Agreement with the experimental results in the rare-earth case was found by assuming a polarization that was spatially uniform but required that  $J_{4f-6s}$  be

TABLE I. A comparison of certain of the magnetic properties of three  $XAl_2$  metals. For the rare-earth metals  $J$  ( $\mathbf{J}=\mathbf{L}+\mathbf{S}$ ) and  $J_z$  are good quantum numbers.  $S_z$  is obtained from the relation  $(J_z/J_z)|S_z|J_z\rangle = J_z(\mathbf{S}\cdot\mathbf{J})/J(J+1)$ . Thus, the change in sign of  $\Delta K/\Delta\chi_{mol}$  for  $PrAl_2$  relative to  $GdAl_2$  arises from the difference in sign of  $\langle\mathbf{S}\cdot\mathbf{J}\rangle$ , depending on whether the  $4f$  shell is less than half-filled or not. The sign of the *spin* polarization at the aluminum site relative to that at the magnetic site in each case is also given.

	$PrAl_2$	$GdAl_2$	$UAl_2$
Character of magnetic electrons	$4f$ (localized)	$4f$ (localized)	$5f$ (band)
$J_z$	$\uparrow$	$\uparrow$	$\dots$
$S_z$	$\downarrow$	$\uparrow$	$\uparrow$
$s_z$ (Al site)	$\uparrow$	$\downarrow$	$\uparrow$
$\Delta K/\Delta\chi_{mol}$	0.82	-0.32	3.8

*negative*.<sup>1,2</sup> It has been suggested that this dilemma has its origin in the fact that the polarization induced in the  $s$  conduction band by the  $f$ - $s$  exchange interaction is decidedly not uniform even in a dense magnetic material like  $GdAl_2$  (see discussion in reference 2). Recently Yosida<sup>20</sup> has calculated the polarization for  $GdAl_2$ , treating the conduction electrons in the free-electron approximation with an assumed  $q$  (wave number) dependence of the exchange interaction which is constant for  $q \leq 2k_F$  and vanishes for  $q > 2k_F$ . He has found the spin density in the conduction band at the Al position opposite to that at the Gd position. This range of  $q$  for  $J(q)$  roughly corresponds to a range in position equal to that of the radius of the  $4f$  shell. However, in the case of  $UAl_2$ , where the spatial extent of the  $5f$  electrons is considerably greater, the range in  $q$  of  $J(q)$  will be appreciably *decreased*. This has the effect of reducing the spatial variations in the conduction electron polarization. For  $UAl_2$ , we might expect these considerations to lead to a positive spin density at the aluminum site.

It has been convenient in our treatment to consider admixture effects and exchange polarization as alternative descriptions of a single physical phenomenon. More likely both effects exist simultaneously and contribute independently to the observed result. For the local magnetic ion-conduction electron case this point of view has been advanced by Anderson and Clogston<sup>21</sup> with particular regard to the manganese in copper problem.

### 3. Large Contribution to the Temperature-Independent Susceptibility

A striking feature of  $K$  vs  $\chi$  plot is the extrapolated intercept on the  $\chi$  axis corresponding to  $K=0$ . To properly interpret this, we must first correct for the contribution to  $K$  arising from  $\chi_s$ . There will also be a contribution that is temperature independent arising from an admixture of Al  $3s$  wave function into the  $6d$  band. The simplest assumption to make is that the

<sup>17</sup> M. Shimizu, J. Phys. Soc. Japan **16**, 1114 (1961).

<sup>18</sup> A. M. Clogston (unpublished private communication).

<sup>19</sup> G. Lehmann, Phys. Rev. **116**, 846 (1959).

<sup>20</sup> K. Yosida (private communication).

<sup>21</sup> P. W. Anderson and A. M. Clogston, Bull. Am. Phys. Soc. (to be published).

fractional admixture of  $3s$  wave function into the  $5f$  and  $6d$  bands to be the same, i.e.,  $f_{3s,6d} = f_{3s,5f}$  and the remaining fraction  $(1 - 2f_{3s,5f})$  to be the amount of Al  $3s$  in the  $7s$  band. Again only  $\chi_f(T)$  is assumed temperature dependent. This is schematicized in Fig. 6.

The large residual susceptibility corresponding to the intercept on the  $\chi$  axis at  $K=0$  still has to be explained. We believe its origin is to be found in the analog in metals to the Van Vleck temperature-independent paramagnetism. The theory of this has been given by Kubo and Obata.<sup>22</sup> In a partially filled band matrix elements exist, that are linear in the applied field, of the components of the angular momentum between states (which for  $k=0$  are initially degenerate) in the occupied parts of the band and those in the unoccupied parts of the band. The magnitude of the orbital paramagnetism does not depend on the density of states at the Fermi surface but rather on the mean separation  $\Delta$  of the "degenerate" levels and would not be particularly temperature dependent even for a narrow band. The unenhanced (by exchange) spin susceptibility of the  $5f$  electrons is, at  $T=0^\circ\text{K}$ ,  $\chi_f^s = 2\mu_B^2 n(E_F)$ , and the magnitude of the Kubo-Obata orbital paramagnetism is  $\chi_f^{\text{orb}} = 2\mu_B^2 N | \langle 0 | L_z | i \rangle |_{\text{av}}^2 / \Delta$ , where  $N$  is the number of  $5f$  electrons per  $U$  atom in the filled part of the band. Since the orbital paramagnetism of the  $U$   $5f$  electrons corresponds to circulating moments centered on each  $U$  atom the fields produced are localized to the  $U$  atoms and therefore do not contribute to the Knight shift at the Al sites.<sup>23</sup>

The observed intercept yields a value of  $\chi^{\text{orb}} \approx 3 \times 10^{-6}$  emu/g which, using the order of magnitude expression for  $\chi^{\text{orb}}$ , predicts a  $\Delta \approx 0.37$  eV if we take  $N=2$  and  $| \langle 0 | L_z | i \rangle |_{\text{av}}^2 = 2$ . If we assume there is no exchange contribution to the susceptibility of the  $f$  electrons so that we may associate the maximum in the susceptibility  $\chi_f^s, \text{max}$  with the  $n_f(E_F)$  we may calculate the width  $\delta$  of the  $5f$  sub-band. (See Reference 16, p. 1360.) If it takes approximately four electrons to completely fill this sub-band and there are 8 U + 16 Al atoms in the

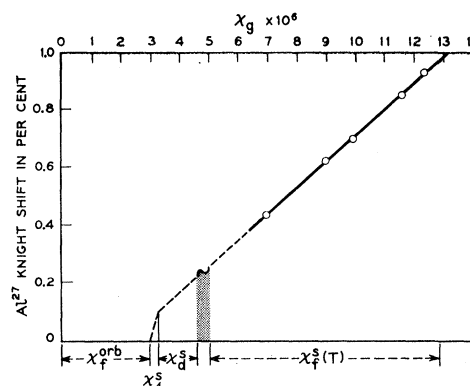


FIG. 6. The  $\text{Al}^{27}$  Knight shift vs susceptibility for  $\text{UAl}_2$  with the separate contributions to  $K$  and  $\chi$  delineated. The shaded area is meant to indicate an uncertainty in the magnitude of the temperature-independent  $d$  and/or  $f$  contribution to the susceptibility.

unit cell, then it will require 32  $f$  electrons per unit cell. Then  $\delta$  is given by

$$\delta = \frac{32}{(M_0/\mu_B^2)(8M_U + 16M_{\text{Al}})} \chi_f^s, \text{max},$$

which yields a value of  $\delta = 0.057$  eV if we take  $(\chi_f^s)_{\text{max}} = 8 \times 10^{-16}$  emu/g. Though the estimates of  $\delta$  and  $\Delta$  admittedly are crude, their relative magnitudes indicate that an appreciable part of  $\chi_f^{\text{orb}}$  comes from states not contained within the narrow peak in the  $f$  band that is responsible for the large  $\chi_f^s$ . It would be extremely useful to have independent corroborating evidence from measurements of specific heat, etc.<sup>24</sup>

#### ACKNOWLEDGMENTS

We are indebted to H. J. Williams and R. C. Sherwood for the measurements of the susceptibility and to J. L. Davis for assistance with the NMR measurements. We wish to thank A. M. Clogston, M. Peter, and Y. Yafet for several discussions.

<sup>22</sup> R. Kubo and Y. Obata, J. Phys. Soc. Japan **11**, 547 (1956).

<sup>23</sup> A study of the Kubo-Obata contribution to the Knight shifts and susceptibilities in  $d$ -group metals and intermetallic compounds has been made. A. M. Clogston, A. C. Gossard, V. Jaccarino, and Y. Yafet, Phys. Rev. Letters **9**, 262 (1962).

<sup>24</sup> Note added in proof. The electronic specific heat of  $\text{UAl}_2$  has been determined at low temperatures (1.4 to  $20^\circ\text{K}$ ), yielding a value of  $\gamma \approx 210 \times 10^{-4}$  cal mole<sup>-1</sup> deg<sup>-2</sup>. Not only does this support the model we have proposed but it is interesting to note that this is the largest value of  $\gamma$  found to date. We are indebted to J. Maity for performing this measurement for us.